

# Irisin suppresses PDGF-BB-induced proliferation of vascular smooth muscle cells *in vitro* by activating AMPK/mTOR-mediated autophagy

Fenqiang Qi,<sup>1</sup> Yuxin Deng,<sup>1</sup> Wei Huang,<sup>1</sup> Yanli Cai,<sup>2</sup> Kelin Hong,<sup>2</sup> Shui Xiang<sup>1,2</sup>

<sup>1</sup>Department of Cardiothoracic Surgery, Liuzhou Worker's Hospital, Liuzhou

<sup>2</sup>Department of Cardiothoracic Surgery, The Central Hospital of Enshi Tujia and Miao Autonomous Prefecture, Enshi, China

## ABSTRACT

Restenosis is a pivotal factor that restricts the efficacy of coronary artery bypass grafting. Inhibition of vascular smooth muscle cells (VSMCs) proliferation can improve intimal hyperplasia and lumen stenosis. Irisin, a polypeptide secreted by muscle cells, has been demonstrated to have a protective role in various cardiovascular diseases. However, the effect and mechanism of irisin on VSMCs proliferation and phenotype switching remain unclear. Cell proliferation ability was assessed using the methylthiazolyldiphenyl-tetrazolium bromide (MTT) assay and 5-ethynyl-2'-deoxyuridine (EdU) incorporation. Cell cycle analysis was performed using flow cytometry, while expression levels of contractile and synthesis-related proteins were determined through RT-qPCR and Western blot. The VSMCs were infected with an adenovirus carrying GFP-LC3, and the proportion of cells showing positive expression was assessed. Additionally, the formation of autophagic lysosomes in cells was observed through transmission electron microscopy. In this study, we have demonstrated the inhibitory effects of irisin on the proliferation and phenotypic transition of platelet-derived growth factor-BB (PDGF-BB)-induced VSMCs. More importantly, we have discovered that irisin can activate the AMP-activated protein kinase/mammalian target of rapamycin (AMPK/mTOR) signaling pathway to mediate autophagy in PDGF-BB-induced VSMCs. The inhibitory effect of irisin on PDGF-BB-induced VSMCs proliferation was significantly attenuated by the AMPK inhibitor, Compound C. Conversely the mTOR inhibitor, rapamycin further enhanced the inhibitory effect of irisin on PDGF-BB induced VSMCs proliferation. In conclusion, our findings suggest that irisin effectively suppresses the aberrant proliferation of VSMCs following PDGF-BB stimulation by modulating autophagy levels through the AMPK/mTOR signaling pathway.

**Key words:** vascular smooth muscle cells; irisin; cell proliferation; autophagy; AMPK/mTOR signaling pathway.

**Correspondence:** Shui Xiang, Department of Cardiothoracic Surgery, Liuzhou Worker's Hospital, No. 156 Heping Road, Liunan District, Liuzhou 545007, Guangxi Province, China. Tel. +86.15971715097.  
E-mail: 15971715097@163.com

**Contributions:** FQ, YD, performed the experiments and analyzed the data; FQ, drafted the manuscript; WH, YC, revised the manuscript and visualized figures; KH performed the statistical analyses; SX, contributed to the study design, literature research, manuscript review. All authors read and approved the final version of the manuscript and agreed to be accountable for all aspects of the work.

**Conflict of interest:** the authors have no potential conflict of interest to declare.

**Ethics approval:** not applicable.

**Data availability:** the data that support the findings of this study are available from the corresponding author upon reasonable request.

**Funding:** this work was supported by the Science and Technology Plan Project of Enshi Tujia and Miao Autonomous Prefecture (No. D2020006).

## Introduction

Coronary heart disease (CHD) is a kind of cardiovascular disease caused by atherosclerosis, thromboembolism and other factors leading to vascular stenosis or even obstruction. In recent decades, there has been a rapid increase in the incidence and mortality rates of CHD in China.<sup>1</sup> CHD not only poses a significant threat to human health and diminishes quality of life but also imposes a substantial economic burden.<sup>2,3</sup> The coronary artery bypass graft (CABG) is widely employed for the treatment of coronary artery diseases.<sup>4</sup> Despite its proven therapeutic efficacy in patients with CHD, ensuring graft patency remains a crucial factor in achieving optimal therapeutic outcomes.<sup>5</sup> The great saphenous vein remains the primary conduit for CABG due to its ease of harvest, excellent controllability, and high flow capacity. However, the long-term patency rate of the saphenous vein following CABG is only 40-50% at 10 years, significantly impacting both mid- and long-term prognoses.<sup>5</sup> Therefore, identification of the key molecular mechanism underlying vein graft restenosis (VGR) after CABG and the development of targeted strategies for its prevention and treatment are crucial for enhancing the prognosis of patients following CABG. Currently, intimal hyperplasia caused by the proliferation and migration of vascular smooth muscle cells (VSMCs) is widely acknowledged as the primary mechanism underlying VGR.<sup>6</sup> However, the pathophysiological mechanisms involved in VGR are complex and still not fully understood. Endothelial cell dysfunction, platelet activation, macrophage aggregation, inflammatory cytokine secretion, and a variety of pathophysiological processes promote VSMCs from contractile phenotype to synthetic phenotype, migration to the intima and proliferation, increased synthesis and secretion of extracellular matrix and deposition in the intima, eventually leading to intimal hyperplasia and lumen stenosis.<sup>7</sup> Our previous animal study also demonstrated an upregulation of various inflammatory cytokines expression at 1 week post vein grafting, along with the observation of T cell and macrophage infiltration in the hyperplastic intima at 2-4 weeks after transplantation.<sup>8</sup> The inhibition of VSMCs proliferation and migration induced by inflammation may represent a potential therapeutic approach to enhance vascular graft patency.

The process of autophagy serves as a vital physiological defense mechanism, relying on the degradative capability of lysosomes to counteract diverse pathological stimuli. It assumes a pivotal role in preserving cellular architecture, functionality, and metabolic equilibrium.<sup>9</sup> Autophagy is also crucial in the regulation of inflammation: research has demonstrated that impaired autophagy in macrophages exacerbates vascular inflammation in mice with atherosclerosis, whereas conversely, augmented autophagy suppresses inflammation.<sup>10</sup> The AMP-activated protein kinase/ mammalian target of rapamycin (AMPK/mTOR) signaling pathway has been extensively studied and demonstrated to play a pivotal role in the regulation of cellular autophagy.<sup>11-13</sup> The previous studies have demonstrated that the upregulation of the AMPK/mTOR autophagy pathway can effectively reduce lipid deposition in vascular walls<sup>14</sup> and inhibit proliferation of VSMCs,<sup>15</sup> thereby exerting significant anti-atherosclerotic effects. Therefore, targeting the AMPK/mTOR autophagy pathway may hold significant promise for the prevention and treatment of VGR.

The myogenic factor, irisin, was discovered in 2012 as a polypeptide generated through proteolytic cleavage of the extracellular domain of fibronectin type III domain-containing protein 5 (FNDC5).<sup>16</sup> The recent years have witnessed a growing body of evidence suggesting that irisin exerts its effects on atherosclerosis,<sup>17</sup> myocardial ischemia/reperfusion injury,<sup>18</sup> ventricular remodeling,<sup>19</sup> and other cardiovascular diseases through its anti-inflammatory properties and enhancement of energy metabolism.

Moreover, the activation of the AMPK/mTOR pathway by irisin induces autophagy,<sup>20</sup> anti-inflammatory responses, and antioxidative stress mechanisms,<sup>21</sup> thereby effectively regulating cellular proliferation, apoptosis, and other biological processes. However, the impact of irisin on VSMCs phenotype switching, proliferation, and intimal hyperplasia remains uncertain in relation to its potential role in promoting autophagy through activation of the AMPK/mTOR pathway. Therefore, the objective of this study was to investigate the role and potential molecular mechanism of irisin in regulating VSMCs proliferation, with the aim of providing novel insights for the prevention and treatment of VGR.

## Materials and Methods

### Reagents

Rat thoracic aorta VSMC line A7R5 were provided by the Cell Bank of China Center for Type Culture Collection. Irisin and propidium iodide (PI) were purchased from Sigma-Aldrich (St. Louis, MO, USA). Dulbecco's Modified Eagle's Medium (DMEM) was purchased from Procell (Wuhan, China). Fetal bovine serum (FBS) was procured from ExcellBio (Shanghai, China). Platelet derived growth factor-BB (PDGF-BB) was purchased from Pepro Tech (Rocky Hill, CT, USA). Compound C and rapamycin were purchased from MedChem Express (Monmouth Junction, NJ, USA). Methylthiazolyldiphenyl-tetrazolium bromide (MTT) cell proliferation and cytotoxicity assay kit, 5-ethynyl-2'-deoxyuridine (EdU) cell proliferation kit with Alexa Fluor 594, 0.3% TritonX-100, Hoechst 33342 solution, and RIPA lysate were purchased from Beyotime (Shanghai, China). GFP-LC3 adenovirus were supplied by Genechem (Shanghai, China). Polyvinylidene difluoride (PVDF) membrane was purchased from Millipore (Billerica, MA, USA). The anti-alpha-smooth muscle actin ( $\alpha$ -SMA) antibody was purchased from Affinity (Jiangsu, China). The antibodies against smooth muscle 22-alpha (SM22- $\alpha$ ), h1-calponin, cellular retinol binding protein-1 (CRBP-1), matrix metalloproteinase-2 (MMP-2), Collagen III, and AMPK were purchased from Proteintech (Wuhan, China). Matrix metalloproteinase-9 (MMP-9) antibody was purchased from Bioss (Beijing, China). The anti-Collagen I antibody was purchased from NOVUS (Littleton, CO, USA). The antibodies recognizing phospho-AMPK (Thr172), mTOR, phospho-mTOR (Ser2448), and microtubule-associated protein 1 lightchain 3B (LC3B) were purchased from Cell Signaling Technology (Danvers, MA, USA). The anti-P62 antibody was purchased from ABclonal (Wuhan, China). The anti-GAPDH antibody was purchased from Goodhere (Hangzhou, China). HRP labeled goat anti-rabbit and mouse secondary antibodies were purchased from Boster (Wuhan, China).

### Cell culture and treatment

The A7R5 cells were cultured in DMEM supplemented with 10% FBS under atmosphere at 37°C with 5% CO<sub>2</sub>. Group intervention was initiated when the cell confluence reached approximately 70%. The A7R5 cells were pre-exposed to irisin (1 mg/L), the AMPK pathway inhibitor Compound C (10  $\mu$ mol/L), or the mTOR inhibitor rapamycin (2 mg/L) for a duration of 30 min. Subsequently, they were treated with PDGF-BB at a concentration of 50 ng/mL for a period of 24 h.<sup>22</sup>

### MTT assay

The cells were seeded at a density of  $3 \times 10^3$  cells/well in 96-well plates and incubated overnight at 37°C, and then divided into different groups (1, treated with 0.1, 0.5, 1.0, 2.5, 5, 10, 20 or 40

mg/L irisin for 24 h; 2, the cells were treated with irisin, Compound C and rapamycin for 30 min followed by PDGF-BB induction for 24 h). 10  $\mu$ L of MTT solution was added to each well and incubated for 4 h at 37°C. Subsequently, 150  $\mu$ L of dimethyl sulfoxide was added and the mixture was shaken for 10 min. The cell proliferation activity was determined by measuring the absorbance at 568 nm using a microplate reader (Bio-Rad Laboratories, Hercules, CA, USA).

### EdU incorporation assay

The cell density was adjusted, and  $5 \times 10^5$  cells/well were seeded onto coverslips in 6-well plates. The cells were synchronized by culturing them in serum-free DMEM for 24 h, followed by culture in DMEM containing 10% FBS for another 24 h. The cells were grouped and subjected to treatment with irisin, Compound C, and rapamycin, respectively. Subsequently, they were stimulated with PDGF-BB for a duration of 24 h. The EdU was added and incubated for 2 h. The cells were fixed with 4% paraformaldehyde at room temperature for 15 min. Subsequently, the cells were incubated with phosphate buffer saline (PBS) containing 0.3% TritonX-100 for 15 min at room temperature. Subsequently, the cells were treated with the Click reaction solution, followed by incubation in the dark for 30 min. Next, Hoechst 33342 solution was added and incubated at room temperature in the dark for 10 min. The coverslips were removed and the cell staining was examined using a fluorescence microscope (Olympus, Tokyo, Japan). The EdU positive index was determined by counting the number of EdU-positive cells and the total number of cells in five randomly selected fields for each sample.

### Flow cytometric assay

The A7R5 cells in the logarithmic growth phase were harvested, and their cell density was adjusted. Subsequently, the cells were seeded at a density of  $5 \times 10^5$  cells/well in 6-well plates and cultured overnight at 37°C. The cells were grouped and subjected to treatment with irisin, Compound C, and rapamycin, respectively. Subsequently, they were stimulated with PDGF-BB for a duration of 24 h. The cells were harvested and fixed by addition of ethanol pre-cooled at -4°C. Subsequently, the cells were incubated with 100  $\mu$ L of RNase at a temperature of 37°C for a duration of 30 min, followed by staining with 400  $\mu$ L of PI in the dark at a temperature of 4°C for another 30 min. Finally, flow cytometry (Beckman Coulter, Brea, CA, USA) was employed to detect the distribution of cell cycle.

### GFP-LC3 adenovirus infection

The A7R5 cells in the logarithmic growth phase were harvested, and their cell density was adjusted. Subsequently, they were seeded at a concentration of  $3 \times 10^3$  cells/well in 96-well plates and cultured overnight at 37°C. The GFP-LC3 adenovirus stock was diluted with serum-free DMEM according to the number of cells and multiplicity of infection (MOI = 40). Subsequently, the appropriate dose of virus dilution was added to each well, mixed thoroughly, and incubated at 37°C for 12 h. After removing the culture medium and introducing different drugs, the cells were harvested, and the cellular LC3 level was examined using a fluorescence microscope. Five random fields were selected to count the number of cells with bright green fluorescent spots and the total number of cells, and then the rate of GFP-LC3 positive cells was calculated.

### Transmission electron microscopy analysis

The A7R5 cells were harvested and seeded in 6-well plates, followed by overnight culture at 37°C. Subsequently, the cells were divided into groups and treated with different drugs. After treatment, the cells in each group were collected, washed with PBS, and then fixed with 2.5% glutaraldehyde for 2 h at 4°C. After rinsing the cells with PBS, 1% osmic acid was added and fixation was carried out for 2 h at room temperature. Subsequently, dehydration was performed using a gradient of ethanol, followed by infiltration of the Epon 812 embedding agent into the cells and polymerization for 48 h. The polymerized samples were sectioned into 60 nm-thick ultra-thin sections, sequentially stained with uranyl acetate and lead citrate solution, and ultimately observed under a transmission electron microscopy (TEM) (Hitachi, Tokyo, Japan).

### RT-qPCR

The A7R5 cells from each group were collected, mixed with 1 mL of Trizol reagent, and lysed for 10 min. Subsequently, the purity and concentration of total RNA were determined after extraction and stored at -80°C for future use. The reverse transcription was carried out using HiScript® II Q Select RT SuperMix for qPCR for cDNA synthesis, followed by RT-qPCR using qPCR SYBR Green Master Mix. The reaction program consisted of a pre-denaturation step at 95°C for 10 min and 40 cycles: Denaturation at 95°C for 15 s, followed by annealing and extension at 60°C for 60 s. The primers utilized in this investigation were supplied by Beijing Tsingke Biotech Co., Ltd., with the specific sequences shown in Table 1.

**Table 1.** Primer sequences for RT-qPCR.

Gene	Primer	Sequence (5'-3')	Product length (bp)
GAPDH	Forward	CAGCAACAGGGTGGTGGAC	253
	Reverse	TTTGAGGGTGCAGCGAACTT	
$\alpha$ -SMA	Forward	CAGAAATACGACCACCAGCG	235
	Reverse	ACCTTCTTCACAGATCCCGG	
SM22- $\alpha$	Forward	ATTGTAATGCAGTGTGGCCC	189
	Reverse	TTGAGCCACCTGTCCATCT	
Calponin h1	Forward	CAGAAATACGACCACCAGCG	155
	Reverse	ACCTTCTTCACAGATCCCGG	
CRBP-1	Forward	CCTGTGGACTTCAACGGGTA	214
	Reverse	CCTCGAACTCCTTCCCAACT	
MMP-2	Forward	CCAAGAACTTCCGACTATCCA	217
	Reverse	GTCAGTGTCCGCAAATAAA	
MMP-9	Forward	GCTGGGCTTAGATCATTCTTCAGTG	109
	Reverse	CAGATGCTGGATGCCTTTTATGTCTG	
Collagen	Forward	CGATCCTGCCGATGTGCTATCC	246
	Reverse	GTCTTGCCCCAAGTCCGGTGTG	
Collagen	Forward	TTTGTGCAATGTGGGACCTG	236
	Reverse	TTTGTGCAATGTGGGACCTG	

## Western blot

The A7R5 cells from each group were collected and lysed on ice for 30 min with the addition of RIPA lysate. Subsequently, the cells were centrifuged at 12000 rpm for 5 min at 4°C, and the resulting supernatant was collected to determine protein concentration. The protein solution was denatured in boiling water and subjected to electrophoresis using a 5% concentrate gel and a 12% separation gel to separate the proteins. Gels containing target protein bands were excised and transferred onto PVDF membranes. These membranes were then blocked with a blocking solution containing 5% skim milk powder for a duration of 2 h. The membranes were incubated overnight at 4°C with primary antibodies recognizing  $\alpha$ -SMA, SM22- $\alpha$ , CRBP-1, h1-calponin, MMP-2, MMP-9, Collagen I, Collagen III, AMPK, p- AMPK, mTOR, p- mTOR, LC3B, P62, or GAPDH (dilution 1:1000). Subsequently, the membranes were further incubated for 2 h at room temperature with the appropriate secondary antibodies (dilution 1:10000). Finally, chemiluminescence reagents were dropped onto the membrane and reacted for 1 min. The gray value of protein bands was measured using Image J software, followed by conducting statistical analysis.

## Statistical analysis

SPSS 23.0 software was used for statistical analysis. All experiments were performed in triplicate, and data were given as means  $\pm$  SD. The one-way analysis of variance (ANOVA) was used for comparisons of multiple groups, while the least significant differ-

ence (LSD) test was utilized for pairwise comparisons between groups. Statistical significance was determined at a threshold of  $p < 0.05$ .

## Results

### Irisin inhibits PDGF-BB-induced cell proliferation in VSMCs

First, we tested the toxic effect of irisin on VSMCs and found that concentrations of irisin equal to or lower than 5 mg/L did not significantly impact the proliferation activity of VSMCs (Figure 1A). The results of MTT assay demonstrated that the induction of PDGF-BB could effectively enhance the proliferation of VSMCs. However, treatment with irisin at concentrations of 1, 2.5, and 5 mg/L significantly suppressed the proliferation of VSMCs induced by PDGF-BB, with no significant difference observed among these three concentrations (Figure 1B). Therefore, a concentration of irisin was chosen as 1 mg/L for subsequent experiments. Consistent with the results of the MTT assay, the EdU incorporation assay also demonstrated that VSMCs proliferation was enhanced by PDGF-BB induction, while irisin treatment effectively suppressed PDGF-BB- induced VSMCs proliferation (Figure 1C). Furthermore, we observed that irisin treatment arrested a majority of PDGF-BB- induced VSMCs in the  $G_{0/1}$  phase and

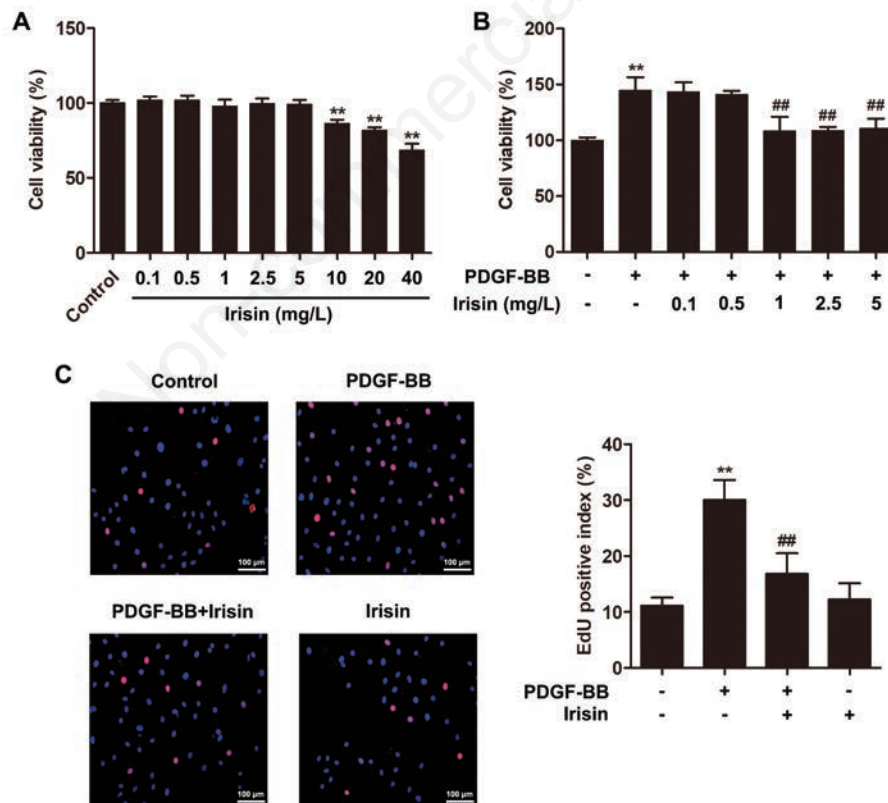


**Figure 1.** Irisin inhibited the proliferation of VSMCs induced by PDGF-BB. **A,B)** The MTT assay was employed to assess the impact of various concentrations of irisin on the proliferation of VSMCs or PDGF-BB-induced VSMCs. **C)** EdU incorporation assay was used to evaluate VSMCs proliferation; red fluorescence indicates EdU-labeled proliferating cells, and blue fluorescence indicates nuclei. Scale bar: 100  $\mu$ m; \*\* $p < 0.01$  compared with control group; ## $p < 0.01$  compared with PDGF-BB group.

attenuated cell entry into S phase, thereby inhibiting cellular proliferation (Figure 2).

### Irisin attenuates PDGF-BB-induced phenotypic switching in VSMCs

The results of RT-qPCR and Western blot analysis demonstrated a significant downregulation in the expression levels of  $\alpha$ -SMA, SM22- $\alpha$ , h1-calponin, and CRBP-1 in VSMCs induced by PDGF-BB (Figure 3 A-C). However, treatment with irisin resulted in an increase in their expression levels. On the contrary, VSMCs induced by PDGF-BB exhibited a substantial upregulation in the expression levels of synthetic proteins MMP-2, MMP-9, Collagen I and Collagen III (Figure 3 D-F). Notably, this upregulation was effectively inhibited upon treatment with irisin.

### Irisin activates AMPK/mTOR-mediated autophagy in PDGF-BB-induced VSMCs

Western blot analysis revealed that the expression of p-AMPK/AMPK and LC3B-II/LC3B-I ratio were significantly reduced in VSMCs treated with PDGF-BB compared to the control group, while the levels of p-mTOR/mTOR and p62 protein were markedly increased (Figure 4). The VSMCs were infected with GFP-LC3 adenovirus, and a reduction in the level of GFP-LC3 positive cells was observed in the PDGF-BB group (Figure 5A), along with a reduction in autophagic lysosomes as confirmed by TEM (Figure 5B). However, following irisin treatment, the AMPK pathway was activated in PDGF-BB-induced VSMCs, leading to an increase in the ratio of LC3B-II/LC3B-I protein, a decrease in p62 protein expression, and an enhancement of GFP-LC3B fluorescence and autophagic lysosomes formation.

### AMPK/mTOR-mediated autophagy is involved in the actions of irisin in regulating PDGF-BB-induced cell proliferation in VSMCs

To confirm the inhibitory effect of irisin on VSMCs proliferation through regulation of the AMPK/mTOR pathway-mediated autophagy, we employed Compound C, an AMPK inhibitor, as an autophagy suppressor and rapamycin, an mTOR inhibitor, as an autophagy enhancer. The results demonstrated that Compound C

effectively reversed the inhibitory impact of irisin treatment on PDGF-BB-induced VSMCs proliferation (Figure 6 A,B), mitigated cell cycle arrest at the G<sub>0</sub>/G<sub>1</sub> phase (Figure 7), diminished autophagic lysosomes formation (Figure 8A) and the protein ratio of LC3B-II/LC3B-I, and upregulated p62 protein expression (Figure 8B). The administration of rapamycin, on the contrary, potentiated the effects of irisin on proliferation, cell cycle progression, and autophagy of PDGF-BB-induced VSMCs.

## Discussion

The VSMCs constitute one of the primary cellular components within the intimal layer of blood vessels. Under physiological circumstances, VSMCs exhibit a contractile phenotype and demonstrate limited proliferative activity.<sup>23</sup> However, in pathological conditions, VSMCs undergo a phenotypic transition from differentiation (contractile phenotype) to dedifferentiation (synthetic phenotype), resulting in impaired vascular function and pathological vascular remodeling.<sup>24</sup> Therefore, the physiological regulation of VSMCs is crucial for VGR. The primary discovery of this study is that irisin treatment has the potential to enhance autophagy through the activation of the AMPK/mTOR signaling pathway, thereby effectively suppressing VSMCs phenotypic switching, proliferation, and other biological behaviors. The findings presented here elucidate the molecular mechanism underlying the protective effect of irisin in VSMCs under pathological conditions.

The occurrence of vascular injury triggers the transformation of VSMCs into synthetic VSMCs characterized by a heightened capacity for proliferation and migration, facilitating the repair process. PDGF-BB was the first growth factor to be discovered as a regulator of VSMC dedifferentiation<sup>25</sup> and is commonly employed as an inducer in experimental studies investigating the characteristics of synthetic phenotypic VSMCs.<sup>26,27</sup> The synthetic VSMCs exhibited reduced expression of contractile proteins, such as  $\alpha$ -SMA, SM22- $\alpha$ , and Calponin 1, while demonstrating increased secretion of collagen, MMPs, and elastin.<sup>28</sup> These changes were responsible for mediating vascular extracellular matrix remodeling. Studies have demonstrated that PDGF-BB can

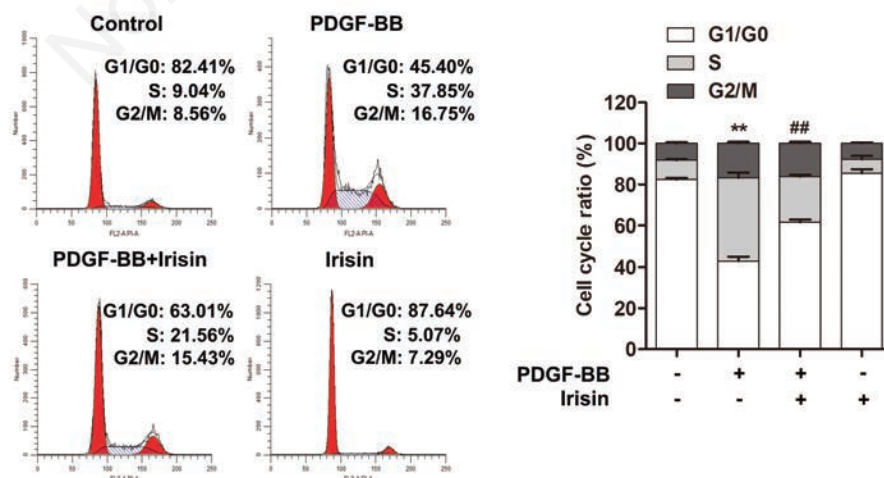


**Figure 2.** Irisin arrested cell cycle progression of VSMCs induced by PDGF-BB. Flow cytometry was used to detect and quantify the cell cycle, and the proportion of cells in G<sub>0</sub>/G<sub>1</sub> phase was statistically analyzed. \*\* $p < 0.01$  compared with control group; ## $p < 0.01$  compared with PDGF-BB group.

enhance the proliferative and migratory activities of VSMCs, while simultaneously suppressing the expression of contractile proteins, thereby inducing phenotypic switch of cells.<sup>29</sup> Consistent with the above reports, in this study, PDGF-BB was employed to induce VSMCs, which exhibited a parallel augmentation in cellular proliferative activity, downregulation of contractile protein expression levels ( $\alpha$ -SMA, SM22- $\alpha$ , h1-calponin and CRBP-1), and upregulation of proteins associated with extracellular matrix synthesis (MMP-2, MMP-9, Collagen I, and Collagen III). At the same time, we also observed that VSMCs autophagy was inhibited,

consistent with previous research findings.<sup>29</sup>

Autophagy is considered a crucial determinant in the process of phenotype switching and cellular stress response in VSMCs. However, autophagy in VSMCs exhibits dual effects on proliferation, and different autophagy inducers yield inconsistent impacts on VSMCs phenotypic switching and proliferation. The findings of previous study have demonstrated that the overexpression of small ubiquitin-related modifier 1 facilitates autophagy, thereby inducing dedifferentiation in VSMCs, ultimately leading to an upregulation in VSMCs proliferation and migration. However, these effects

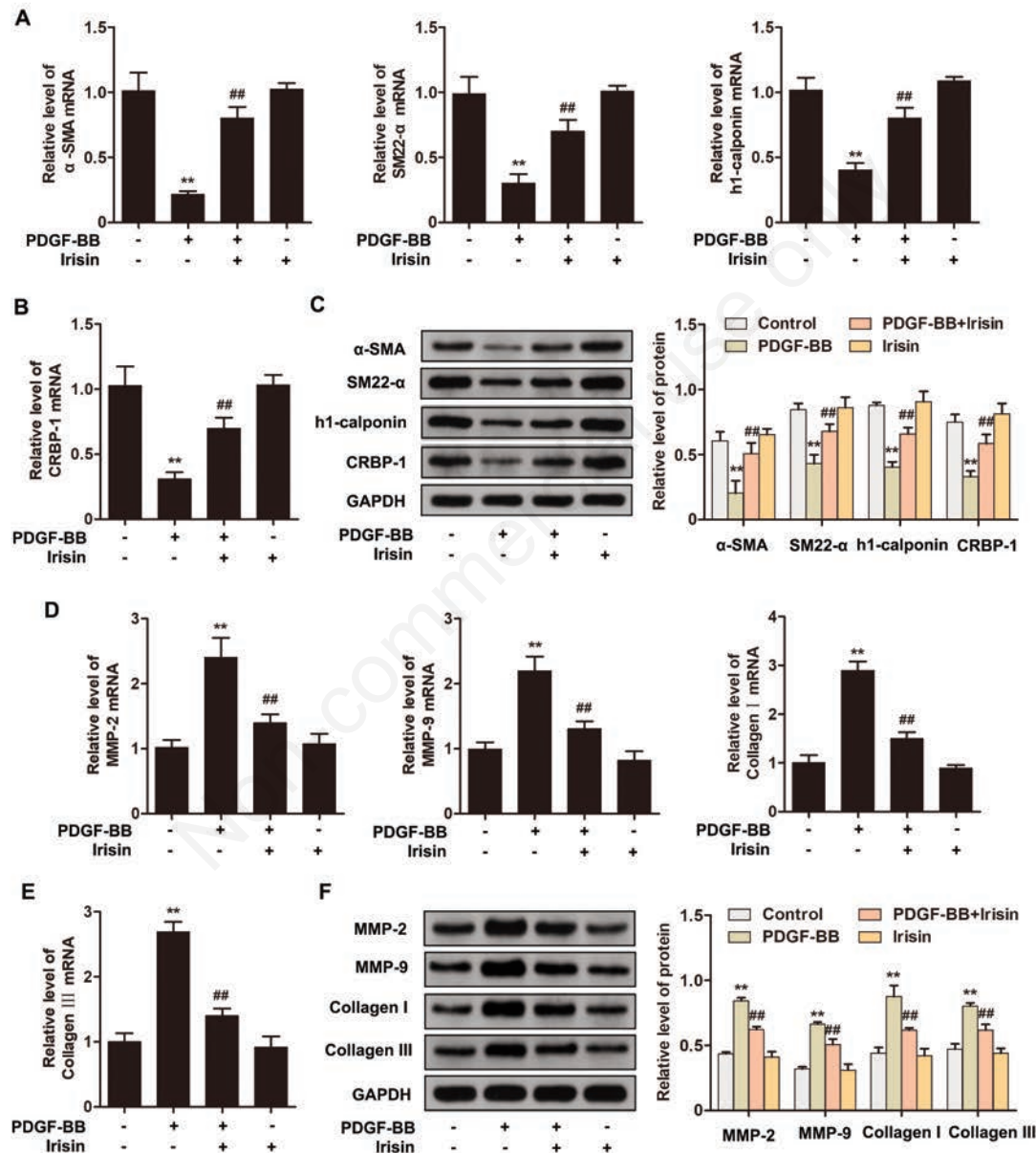


**Figure 3.** Irisin inhibited the phenotypic switching in VSMCs induced by PDGF-BB. **A,B)** RT-qPCR was used to detect the mRNA expression levels of  $\alpha$ -SMA, SM22- $\alpha$ , h1-calponin, and CRBP-1 in VSMCs. **C)** Western blot was used to assess the protein expression levels of  $\alpha$ -SMA, SM22- $\alpha$ , h1-calponin, and CRBP-1 in VSMCs, and quantitative analysis was performed. **D,E)** RT-qPCR was used to detect the mRNA expression levels of MMP-2, MMP-9, Collagen I and Collagen III in VSMCs. **F)** Western blot was used to assess the protein expression levels of MMP-2, MMP-9, Collagen I and Collagen III in VSMCs, and quantitative analysis was performed. \*\* $p < 0.01$  compared with control group; ## $p < 0.01$  compared with PDGF-BB group.

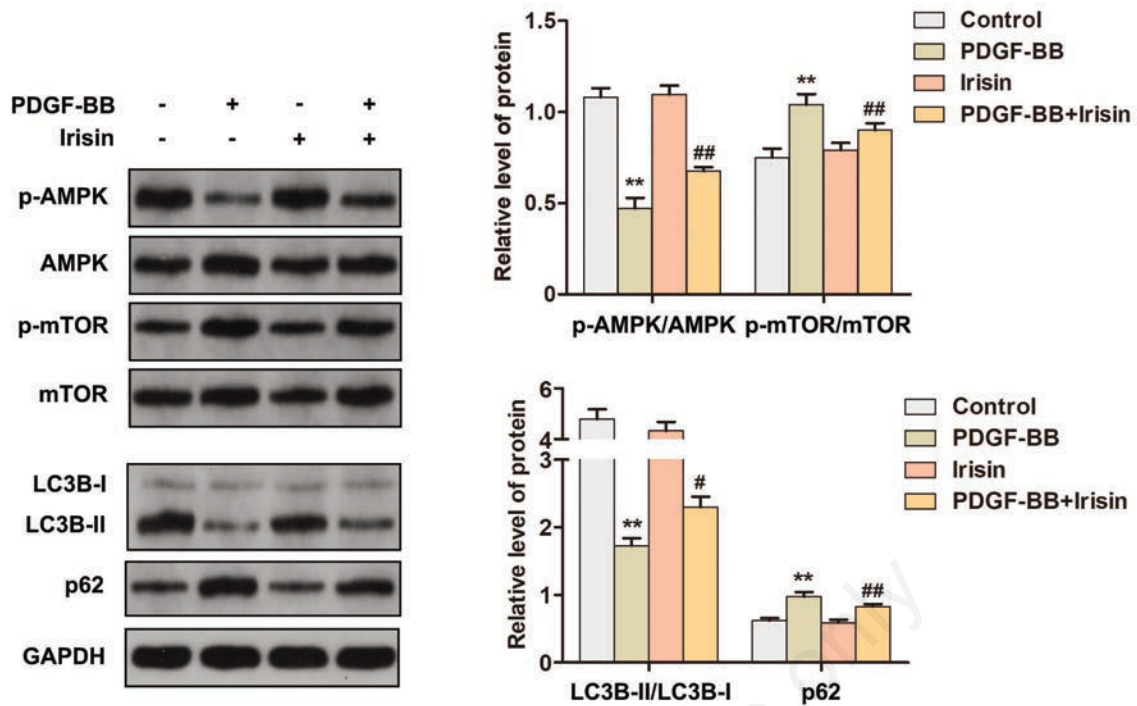


**Figure 4.** Irisin activated AMPK/mTOR-mediated autophagy in PDGF-BB-induced VSMCs. Western blot was used to detect the protein expression levels of p-AMPK, AMPK, p-mTOR, mTOR, LC3B, and p62 in VSMCs, and quantitative analysis was performed. \*\* $p < 0.01$  compared with control group; # $p < 0.05$ , ## $p < 0.01$  compared with PDGF-BB group.

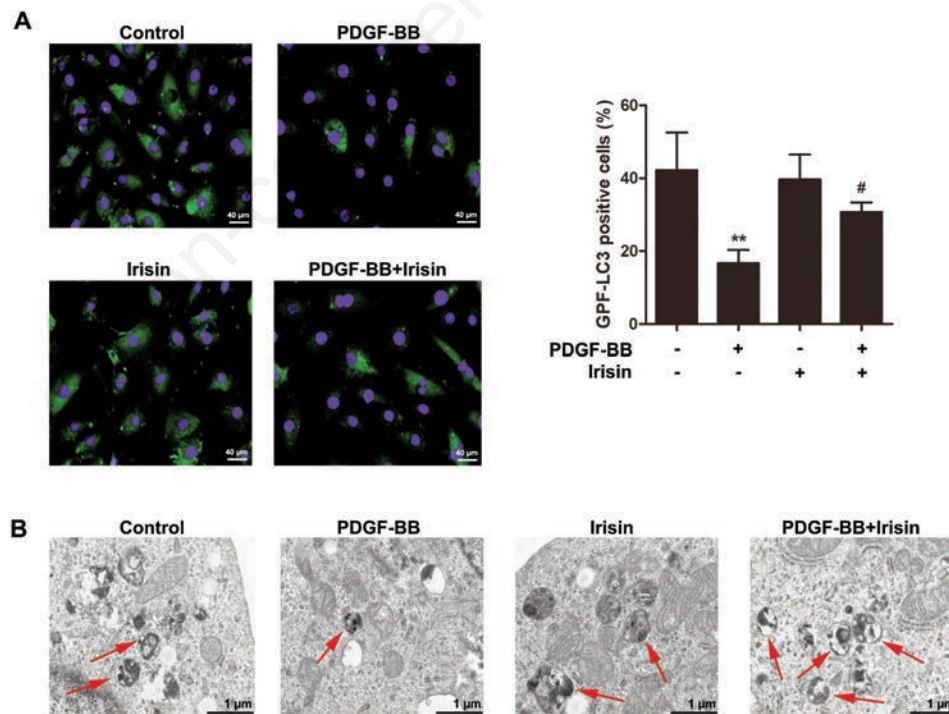


**Figure 5.** Irisin activated autophagy in PDGF-BB-induced VSMCs. **A)** After infecting the VSMCs with GFP-LC3 adenovirus, the presence of green fluorescent spots within the VSMCs was observed and the rate of GFP-LC3 positive cells was quantified; the GFP-LC3 exhibited green fluorescence, while the blue fluorescence originated from the nucleus; scale bar: 40  $\mu\text{m}$ . **B)** Transmission electron microscopy was used to observe the formation of autophagic lysosomes in VSMCs; the autophagic lysosomes were indicated by red arrows; scale bar: 1  $\mu\text{m}$ . \*\* $p < 0.01$  compared with control group; # $p < 0.05$  compared with PDGF-BB group.

can be counteracted by the administration of the autophagy inhibitor 3-methyladenine.<sup>30</sup> Wen *et al.* discovered that the adipokine Chemerin induces proliferation and migration of VSMCs through autophagy.<sup>31</sup> On the contrary, a plethora of findings substantiate the inhibitory role of autophagy in the phenotypic switching of VSMCs. For instance, Fang *et al.* discovered that

methyltransferase-like 3 hampers VSMCs phenotypic transformation through facilitation of autophagosome formation, thereby attenuating cell proliferation and migration.<sup>32</sup> The findings of another study have also indicated that caffeine can induce autophagy, thereby diminishing the proliferation of VSMCs and subsequently reducing the occurrence of vascular restenosis.<sup>33</sup> The

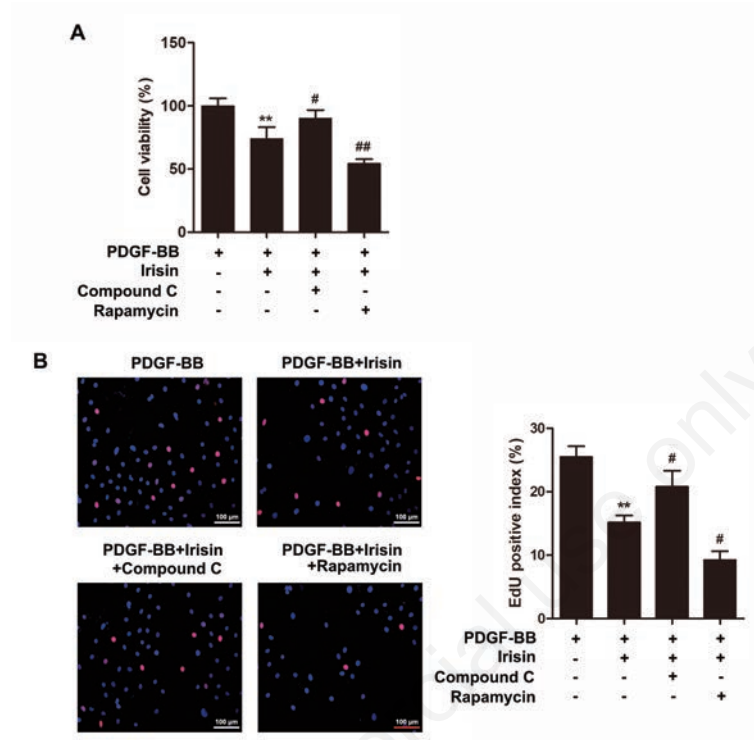


**Figure 6.** Irisin inhibited proliferation of PDGF-BB-induced VSMCs by regulating AMPK/mTOR signaling pathway. **A)** MTT assay was employed to assess VSMCs proliferation activity. **B)** EdU incorporation assay was used to evaluate VSMCs proliferation; scale bar: 100  $\mu$ m. \*\* $p$ <0.01 compared with control group; # $p$ <0.05, ## $p$ <0.01 compared with PDGF-BB group.

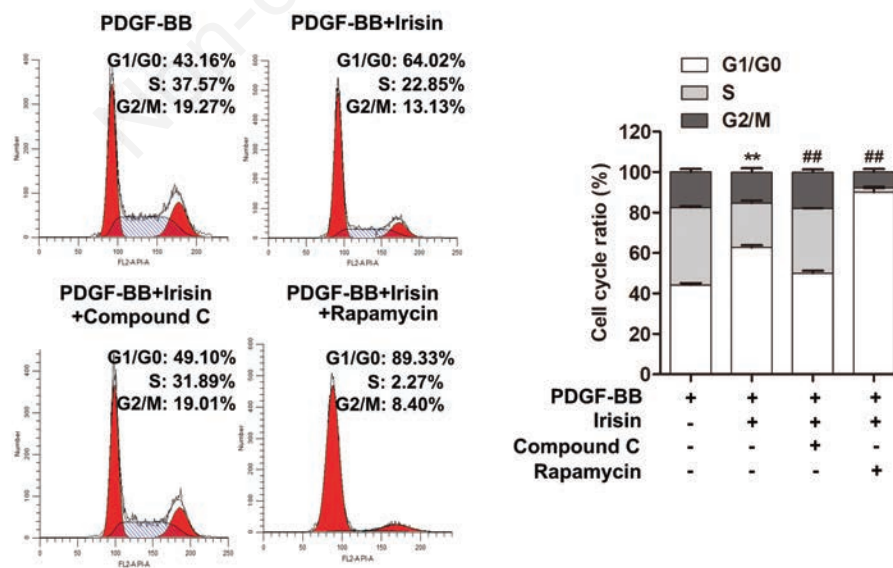


**Figure 7.** Irisin arrested cell cycle progression of PDGF-BB-induced VSMCs by regulating AMPK/mTOR signaling pathway. Flow cytometry was used to detect the cell cycle, and the proportion of cells in G0/G1 phase was statistically analyzed. \*\* $p$ <0.01 compared with control group; ## $p$ <0.01 compared with PDGF-BB group.



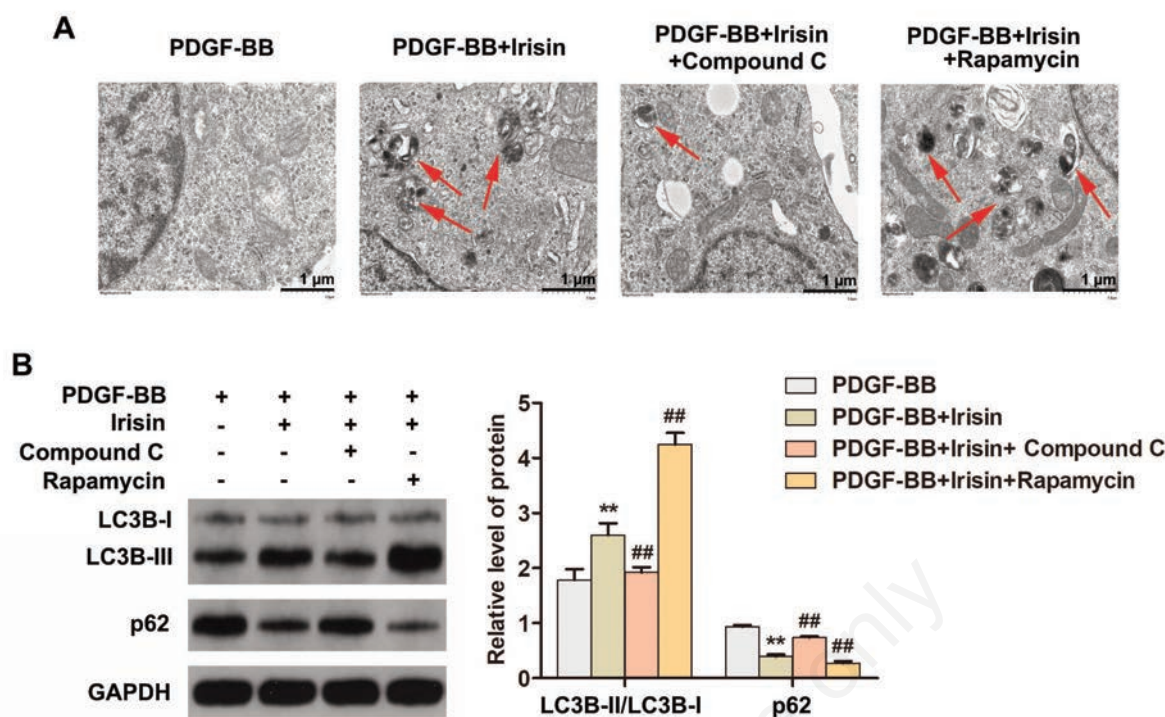


**Figure 8.** Irisin activated autophagy in PDGF-BB-induced VSMCs by regulating AMPK/mTOR signaling pathway. **A)** Transmission electron microscopy was used to observe the formation of autophagic lysosomes in VSMCs. The autophagic lysosomes were indicated by red arrows; scale bar: 1  $\mu$ m. **B)** Western blot was used to detect protein expressions of LC3B and p62, and quantitative analysis was performed. \*\* $p < 0.01$  compared with control group; ## $p < 0.01$  compared with PDGF-BB group.

inconsistent conclusions from these studies may suggest that the degree and molecular mechanism of autophagy vary under different pathological stimuli, leading to diverse effects on VSMCs proliferation. However, it does imply that targeting autophagy could be a critical approach in regulating VSMCs proliferation.

AMPK serves as a crucial cellular energy status sensor, being triggered upon reduction in intracellular ATP production. In response, AMPK is activated to promote catabolic pathways and inhibit anabolic pathways.<sup>34</sup> The activation of AMPK occurs through phosphorylation of Thr172 on the  $\alpha$  subunit by an upstream kinase, and once activated, AMPK can induce autophagy in response to energy stress.<sup>35</sup> mTOR serves as a pivotal regulator at the convergence point of multiple signaling pathways and is subject to negative regulation by AMPK. Research has demonstrated that activation of the AMPK/mTOR-mediated autophagy pathway exerts inhibitory effects on VSMCs proliferation and migration, thereby attenuating intimal hyperplasia following balloon injury.<sup>36</sup> The findings of Hwang *et al.* demonstrated that Far-infrared irradiation effectively mitigated the abnormal proliferation of VSMCs induced by PDGF-BB, potentially through modulation of the AMPK/mTOR signaling axis. Moreover, the therapeutic effect of far-infrared irradiation was significantly reversed upon intervention with an AMPK inhibitor (Compound C).<sup>37</sup> The mTOR inhibitor, rapamycin, has been demonstrated to induce autophagy and elevate autophagic levels in VSMCs, thereby decelerating vascular calcification<sup>38</sup>. The findings of these studies suggest that the AMPK/mTOR signaling pathway plays a crucial role in the regulation of autophagy in VSMCs.

Irisin is a novel hormone secreted by muscle cells, which can promote autophagy through the activation of AMPK and inhibition of mTOR.<sup>20</sup> The potential of irisin as a therapeutic candidate for

cardiovascular diseases is widely recognized, and it has demonstrated the ability to counteract the phenotypic switching and proliferation of VSMCs induced by PDGF-BB.<sup>22</sup> The findings of the present study also demonstrated the regulatory effect of irisin on VSMCs phenotypic switching and proliferation induced by PDGF-BB. However, further clarification is needed to determine whether it affects autophagy by regulating the AMPK/mTOR signaling axis in order to inhibit VSMCs proliferation. The findings of this study demonstrated that treatment with irisin effectively suppressed the proliferation and phenotypic switching of VSMCs induced by PDGF-BB, while simultaneously promoting autophagy. However, the effects of irisin on VSMCs autophagy, proliferation, and cell cycle induced by PDGF-BB were reversed upon addition of Compound C. Conversely, the effectiveness of irisin was further enhanced when rapamycin was introduced.

In conclusion, the findings of this study suggest that irisin may exert inhibitory effects on the abnormal proliferation of VSMCs induced by PDGF-BB through activation of the AMPK/mTOR axis to facilitate autophagy. Although current experimental studies assess autophagy levels based on the abundance of autophagosomes and marker protein expression, there is a lack of definitive biomarkers in clinical research, which also poses challenges for conducting clinical investigations on autophagy.

## References

- Zhu L, Ho SC, Sit JW. The experiences of Chinese patients with coronary heart disease. *J Clin Nurs* 2012;21:476-84.
- Mensah GA, Fuster V, Murray CJL, Roth GA. Global burden

- of cardiovascular diseases and risks, 1990-2022. *J Am Coll Cardiol* 2023;82:2350-473.
3. Mensah GA, Fuster V, Roth GA. A heart-healthy and stroke-free world: Using data to inform global action. *J Am Coll Cardiol* 2023;82:2343-9.
  4. Tsao CW, Aday AW, Almarzooq ZI, Anderson CAM, Arora P, Avery CL, et al. Heart disease and stroke statistics-2023 update: A report from the American Heart Association. *Circulation* 2023;147:e93-e621.
  5. Caliskan E, de Souza DR, Böning A, Liakopoulos OJ, Choi YH, Pepper J, et al. Saphenous vein grafts in contemporary coronary artery bypass graft surgery. *Nat Rev Cardiol* 2020;17:155-69.
  6. Liu X, Qin M, Chen Q, Jiang N, Wang L, Bai Y, Guo Z. Identification of important genes related to HVSMC proliferation and migration in graft restenosis based on WGCNA. *Sci Rep* 2024;14:1237.
  7. de Vries MR, Quax PHA. Inflammation in vein graft disease. *Front Cardiovasc Med* 2018;5:3.
  8. Xiang S, Liu J, Dong N, Shi J, Xiao Y, Wang Y, et al. Suppressor of cytokine signaling 3 is a negative regulator for neointimal hyperplasia of vein graft stenosis. *J Vasc Res* 2014;51:132-43.
  9. Rubio-Tomás T, Sotiriou A, Tavernarakis N. The interplay between selective types of (macro)autophagy: Mitophagy and xenophagy. *Int Rev Cell Mol Biol* 2023;374:129-57.
  10. Wang Z, Gao Z, Zheng Y, Kou J, Song D, Yu X, et al. Melatonin inhibits atherosclerosis progression via galectin-3 downregulation to enhance autophagy and inhibit inflammation. *J Pineal Res* 2023;74:e12855.
  11. Wu N, Ji J, Gou X, Hu P, Cheng Y, Liu Y, et al. DENV-2 NS1 promotes AMPK-LKB1 interaction to activate AMPK/ERK/mTOR signaling pathway to induce autophagy. *Virology* 2023;20:231.
  12. Li T, Tan X, Zhu S, Zhong W, Huang B, Sun J, et al. SPARC induces phenotypic modulation of human brain vascular smooth muscle cells via AMPK/mTOR-mediated autophagy. *Neurosci Lett* 2019;712:134485.
  13. Chen WR, Yang JQ, Liu F, Shen XQ, Zhou YJ. Melatonin attenuates vascular calcification by activating autophagy via an AMPK/mTOR/ULK1 signaling pathway. *Exp Cell Res* 2020;389:111883.
  14. Li BH, Liao SQ, Yin YW, Long CY, Guo L, Cao XJ, et al. Telmisartan-induced PPAR $\gamma$  activity attenuates lipid accumulation in VSMCs via induction of autophagy. *Mol Biol Rep* 2015;42:179-86.
  15. Wu H, Song A, Hu W, Dai M. The anti-atherosclerotic effect of paeonol against vascular smooth muscle cell proliferation by up-regulation of autophagy via the AMPK/mTOR signaling pathway. *Front Pharmacol* 2017;8:948.
  16. Boström P, Wu J, Jedrychowski MP, Korde A, Ye L, Lo JC, et al. A PGC1- $\alpha$ -dependent myokine that drives brown-fat-like development of white fat and thermogenesis. *Nature* 2012;481:463-8.
  17. Zhang Y, Mu Q, Zhou Z, Song H, Zhang Y, Wu F, et al. Protective effect of irisin on atherosclerosis via suppressing oxidized low density lipoprotein induced vascular inflammation and endothelial dysfunction. *PLoS One* 2016;11:e0158038.
  18. Wang Z, Chen K, Han Y, Zhu H, Zhou X, Tan T, et al. Irisin protects heart against ischemia-reperfusion injury through a sod2-dependent mitochondria mechanism. *J Cardiovasc Pharmacol* 2018;72:259-69.
  19. Li RL, Wu SS, Wu Y, Wang XX, Chen HY, Xin JJ, et al. Irisin alleviates pressure overload-induced cardiac hypertrophy by inducing protective autophagy via mTOR-independent activation of the AMPK-ULK1 pathway. *J Mol Cell Cardiol* 2018;121:242-55.
  20. Ma J, Han Z, Jiao R, Yuan G, Ma C, Yan X, Meng A. Irisin ameliorates pm2.5-induced acute lung injury by regulation of autophagy through AMPK/mTOR pathway. *J Inflamm Res* 2023;16:1045-57.
  21. Deng J, Zhang N, Chen F, Yang C, Ning H, Xiao C, et al. Irisin ameliorates high glucose-induced cardiomyocytes injury via AMPK/mTOR signal pathway. *Cell Biol Int* 2020;44:2315-25.
  22. Song H, Xu J, Lv N, Zhang Y, Wu F, Li H, et al. Irisin reverses platelet derived growth factor-BB-induced vascular smooth muscle cells phenotype modulation through STAT3 signaling pathway. *Biochem Biophys Res Commun* 2016;479:139-45.
  23. Xia Y, Zhang X. Mitochondrial homeostasis in vsmcs as a central hub in vascular remodeling. *Int J Mol Sci* 2023;24:3483.
  24. Touyz RM, Alves-Lopes R, Rios FJ, Camargo LL, Anagnostopoulou A, Arner A, Montezano AC. Vascular smooth muscle contraction in hypertension. *Cardiovasc Res* 2018;114:529-39.
  25. Holycross BJ, Blank RS, Thompson MM, Peach MJ, Owens GK. Platelet-derived growth factor-BB-induced suppression of smooth muscle cell differentiation. *Circ Res* 1992;71:1525-32.
  26. Qiu L, Hu L, Liu X, Li W, Zhang X, Xia H, Zhang C. Physalin B inhibits PDGF-BB-induced VSMC proliferation, migration and phenotypic transformation by activating the Nrf2 pathway. *Food Funct* 2021;12:10950-66.
  27. Park ES, Lee KP, Jung SH, Lee DY, Won KJ, Yun YP, Kim B. Compound K, an intestinal metabolite of ginsenosides, inhibits PDGF-BB-induced VSMC proliferation and migration through G1 arrest and attenuates neointimal hyperplasia after arterial injury. *Atherosclerosis* 2013;228:53-60.
  28. Cao G, Xuan X, Hu J, Zhang R, Jin H, Dong H. How vascular smooth muscle cell phenotype switching contributes to vascular disease. *Cell Commun Signal* 2022;20:180.
  29. Song W, Gao K, Huang P, Tang Z, Nie F, Jia S, Guo R. Bazedoxifene inhibits PDGF-BB induced VSMC phenotypic switch via regulating the autophagy level. *Life Sci* 2020;259:118397.
  30. Yao Y, Li H, Da X, He Z, Tang B, Li Y, et al. SUMOylation of Vps34 by SUMO1 promotes phenotypic switching of vascular smooth muscle cells by activating autophagy in pulmonary arterial hypertension. *Pulm Pharmacol Ther* 2019;55:38-49.
  31. Wen J, Wang J, Guo L, Cai W, Wu Y, Chen W, Tang X. Chemerin stimulates aortic smooth muscle cell proliferation and migration via activation of autophagy in VSMCs of metabolic hypertension rats. *Am J Transl Res* 2019;11:1327-42.
  32. Fang ZM, Zhang SM, Luo H, Jiang DS, Huo B, Zhong X, Feng X, et al. Methyltransferase-like 3 suppresses phenotypic switching of vascular smooth muscle cells by activating autophagosome formation. *Cell Prolif* 2023;56:e13386.
  33. Tripathi M, Singh BK, Liehn EA, Lim SY, Tikno K, Castano-Mayan D, et al. Caffeine prevents restenosis and inhibits vascular smooth muscle cell proliferation through the induction of autophagy. *Autophagy* 2022;18:2150-60.
  34. Mihaylova MM, Shaw RJ. The AMPK signalling pathway coordinates cell growth, autophagy and metabolism. *Nat Cell Biol* 2011;13:1016-23.
  35. Hardie DG. AMPK and autophagy get connected. *Embo J* 2011;30:634-5.
  36. Zheng H, Zhai W, Zhong C, Hong Q, Li H, Rui B, et al. Nkx2-3 induces autophagy inhibiting proliferation and migration of vascular smooth muscle cells via AMPK/mTOR signaling pathway. *J Cell Physiol* 2021;236:7342-55.

37. Hwang YJ, Park JH. Far-infrared irradiation decreases proliferation in basal and pdgf-stimulated vsmcs through AMPK-mediated inhibition of mTOR/p70S6K signaling axis. *J Korean Med Sci* 2023;38:e335.
38. Liu Y, Li J, Han Y, Chen Y, Liu L, Lang J, et al. Advanced glycation end-products suppress autophagy by AMPK/mTOR signaling pathway to promote vascular calcification. *Mol Cell Biochem* 2020;471:91-100.

Non-commercial use only

---

Received: 10 July 2024. Accepted: 9 September 2024.

This work is licensed under a Creative Commons Attribution-NonCommercial 4.0 International License (CC BY-NC 4.0).

©Copyright: the Author(s), 2024

Licensee PAGEPress, Italy

*European Journal of Histochemistry* 2024; 68:4104

doi:10.4081/ejh.2024.4104

*Publisher's note: all claims expressed in this article are solely those of the authors and do not necessarily represent those of their affiliated organizations, or those of the publisher, the editors and the reviewers. Any product that may be evaluated in this article or claim that may be made by its manufacturer is not guaranteed or endorsed by the publisher.*